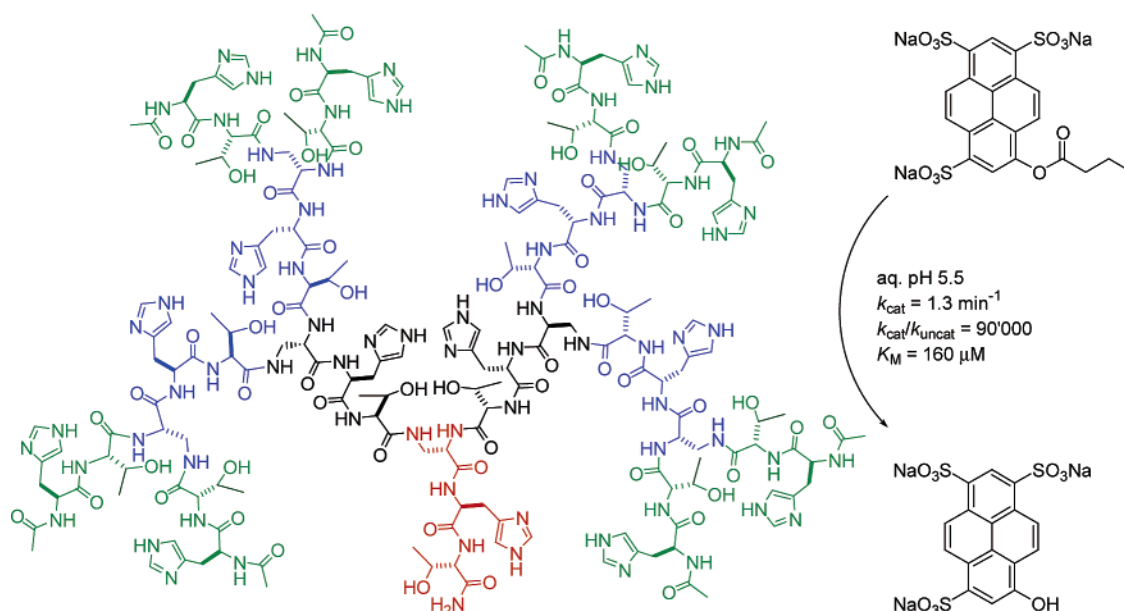


## Synthesis and Activity of Histidine-Containing Catalytic Peptide Dendrimers

Estelle Delort,<sup>†</sup> Nhat-Quang Nguyen-Trung,<sup>‡</sup> Tamis Darbre,<sup>†</sup> and Jean-Louis Reymond<sup>\*,†</sup>  
 Department of Chemistry & Biochemistry, University of Berne, Freiestrasse 3, 3012 Berne, Switzerland,  
 and Chemspeed Technologies AG, Rheinstrasse 32, 4302 Augst, Switzerland  
 jean-louis.reymond@ioc.unibe.ch  
 Received February 9, 2006



Peptide dendrimers built by iteration of the diamino acid dendron Dap-His-Ser (His = histidine, Ser = Serine, Dap = diamino propionic acid) display a strong positive dendritic effect for the catalytic hydrolysis of 8-acyloxypyrene 1,3,6-trisulfonates, which proceeds with enzyme-like kinetics in aqueous medium (Delort, E.; Darbre, T.; Reymond, J.-L. *J. Am. Chem. Soc.* **2004**, *126*, 15642–3). Thirty-two mutants of the original third generation dendrimer **A3** ((Ac-His-Ser)<sub>8</sub>(Dap-His-Ser)<sub>4</sub>(Dap-His-Ser)<sub>2</sub>Dap-His-Ser-NH<sub>2</sub>) were prepared by manual synthesis or by automated synthesis with use of a Chemspeed PSW1100 peptide synthesizer. Dendrimer catalysis was specific for 8-acyloxypyrene 1,3,6-trisulfonates, and there was no activity with other types of esters. While dendrimers with hydrophobic residues at the core and histidine residues at the surface only showed weak activity, exchanging serine residues in dendrimer **A3** against alanine (**A3A**),  $\beta$ -alanine (**A3B**), or threonine (**A3C**) improved catalytic efficiency. Substrate binding was correlated with the total number of histidines per dendrimer, with an average of three histidines per substrate binding site. The catalytic rate constant  $k_{\text{cat}}$  depended on the placement of histidines within the dendrimers and the nature of the other amino acid residues. The fastest catalyst was the threonine mutant **A3C** ((Ac-His-Thr)<sub>8</sub>(Dap-His-Thr)<sub>4</sub>(Dap-His-Thr)<sub>2</sub>Dap-His-Thr-NH<sub>2</sub>), with  $k_{\text{cat}} = 1.3 \text{ min}^{-1}$ ,  $k_{\text{cat}}/k_{\text{uncat}} = 90'000$ ,  $K_{\text{M}} = 160 \mu\text{M}$  for 8-butyryloxypyrene 1,3,6-trisulfonate, corresponding to a rate acceleration of 18'000 per catalytic site and a 5-fold improvement over the original sequence **A3**.

### Introduction

Dendrimers are tree-like molecules with various uses in chemistry and biology, such as catalysis, drug delivery, artificial

vaccines, and gene delivery into cells.<sup>1,2</sup> In the field of catalysis, approaches to dendritic catalysts to date have capitalized on the existence of a dendritic core providing a microenvironment, or on multivalency and size effect accessible by attaching multiple copies of a catalytic group at the dendrimer surface.<sup>3</sup>

Recently we applied the dendritic architecture to synthetic peptides as a strategy to prepare artificial proteins. A dendritic

\* Address correspondence to this author. Fax: +41 31 631 80 57.

<sup>†</sup> University of Berne.

<sup>‡</sup> Chemspeed Technologies AG.

peptide is topologically forced to adopt a globular shape where intramolecular interactions between amino acids are favored over intermolecular interactions leading to aggregation. The dendritic architecture thus circumvents the protein folding problem encountered when designing proteins from linear peptides,<sup>4</sup> which must be addressed with complex combinatorial search algorithms.<sup>5</sup> Dendritic peptides consisting of branched lysine had been investigated previously for multiple antigenic display.<sup>2d,e</sup>

(1) (a) Newkome, G. R.; Moorefield, C. N.; Vögtle, F. *Dendritic Molecules: Concepts, Synthesis, Perspectives*; VCH: Weinheim, Germany, 1996. (b) Newkome, G. R.; Moorefield, C. N.; Vögtle, F. *Dendritic Molecules: Concepts, Synthesis, Applications*; VCH: Weinheim, Germany, 2001. (c) Vögtle, F.; Schalley, C. A., Eds. *Dendrimers V: Functional and Hyperbranched Building Blocks, Photophysical Properties and Applications in Materials and Life Science*; Topics in Current Chemistry, No. 228; Springer-Verlag: Berlin, Germany, 2003. (d) Vögtle, F.; Schalley, C. A., Eds. *Dendrimers IV: Metal Coordination, Self-Assembly and Catalysis*; Topics in Current Chemistry, No. 217, Springer-Verlag: Berlin, Germany, 2001. (e) Tomalia, D. A.; Dvornic, P. R. *Nature* **1994**, *372*, 617–618. (f) Knapen, J. W. J.; van der Made, A. W.; de Wilde, J. C.; van Leeuwen, P. W. N. M.; Wijkens, P.; Grove, D. M.; van Koten, G. *Nature* **1994**, *372*, 659–662. (g) Liang, C.; Fréchet, J. M. J. *Prog. Polym. Sci.* **2005**, *30*, 385–402. (h) Smith, D. K.; *Tetrahedron* **2003**, *59*, 3797–3798. (i) Grayson, S. M.; Fréchet, J. M. J. *Chem. Rev.* **2001**, *101*, 3819–3868. (j) Zeng, F.; Zimmerman, S. C. *Chem. Rev.* **1997**, *97*, 1681–1712.

(2) For peptide dendrimers: (a) Crespo, L.; Sanclimens, G.; Pons, M.; Giralt, E.; Royo, M.; Albericio, F. *Chem. Rev.* **2005**, 1663–1681. (b) Cloninger, M. J. *Curr. Opin. Chem. Biol.* **2002**, *6*, 742–748. (c) Crespo, L.; Sanclimens, G.; Montaner, B.; Pérez-Tomás, R.; Royo, M.; Pons, M.; Albericio, F.; Giralt, E. *J. Am. Chem. Soc.* **2002**, *124*, 8876–8863. (d) Sadler, K.; Tam, J. P. *Rev. Mol. Biotechnol.* **2002**, *90*, 195–229. (e) Tam, J. P.; Lu, Y.-A.; Yang, J.-L. *Eur. J. Biochem.* **2002**, *269*, 923–932. (f) Higashi, N.; Koga, T.; Niwa, M. *ChemBioChem* **2002**, *3*, 448–454. (g) Boas, U.; Sontjens, S. H. M.; Jensen, K. J.; Christensen, J. B.; Meijer, E. W. *ChemBioChem* **2002**, *3*, 433–439. (h) Kinberger, G. A.; Welbo, C.; Goodman, M. J. *J. Am. Chem. Soc.* **2002**, *124*, 15162–15163. (i) Tung, C.-H.; Mueller, S.; Weissleder, R. *Bioorg. Med. Chem.* **2002**, *10*, 3609–3614. (j) Wimmer, N.; Marano, R. J.; Kearns, P. S.; Rakoczy, E. P.; Toth, I. *Bioorg. Med. Chem.* **2002**, *12*, 2635–2637. (k) Lagnoux, D.; Darbre, T.; Schmitz, M. L.; Reymond, J.-L. *Chem., Eur. J.* **2005**, *11*, 3941–3950.

(3) For catalytic dendrimers: (a) Kofoed, J.; Reymond, J.-L. *Curr. Opin. Chem. Biol.* **2005**, *9*, 656–664. (b) Kreiter, R.; Kleij, A. W.; Klein Gebbink, R. J. M.; van Koten, G. *Dendritic Catalysts*; Topics in Current Chemistry, No. 217; Springer-Verlag: Berlin, Germany, 2001; pp 163–199. (c) Twyman, L. J.; King, A. S. H. M.; Martin, I. K. *Chem. Soc. Rev.* **2002**, *31*, 69–82. (d) Astruc, D.; Chardac, F. *Chem. Rev.* **2001**, *101*, 2991–3023. (e) Didier, A.; Heuze, K.; Gatard, S.; Mery, D.; Nlate, S.; Plault, L. *Adv. Synth. Catal.* **2005**, *347*, 329–338. (f) Garcia-Martinez, J. C.; Lezutekong, R.; Crooks, R. M. *J. Am. Chem. Soc.* **2005**, *127*, 5097–5103. (g) Lu, S. M.; Alper, H. *J. Am. Chem. Soc.* **2005**, *127*, 14776–14784. (h) Tang, W.-J.; Yang, N.-F.; Yi, B.; Deng, G.-J.; Huang, Y.-Y.; Fan, Q.-H. *Chem. Commun.* **2004**, 1378–1379. (i) Liang, C. O.; Helms, B.; Craig, J.; Fréchet, J. M. J. *Chem. Commun.* **2003**, 2524–2525. (j) Weyermann, P.; Diederich, F. *Helv. Chim. Acta* **2002**, *85*, 599–617. (k) Liu, L.; Breslow, R. *J. Am. Chem. Soc.* **2003**, *125*, 12110–12111. (l) Bhyrappa, P.; Young, J. K.; Moore, J. S.; Suslick, K. S. *J. Am. Chem. Soc.* **1996**, *118*, 5708–5711.

(4) (a) Haque, T. S.; Little, J. C.; Gellman, S. H. *J. Am. Chem. Soc.* **1994**, *116*, 4105–4106. (b) Raleigh, D. P.; Betz, S. F.; DeGrado, W. F. *J. Am. Chem. Soc.* **1995**, *117*, 7558–7559. (c) Kortemme, T.; Ramirez-Alvarado, M.; Serrano, L. *Science* **1998**, *281*, 253–256. (d) Karle, I. L.; Das, C.; Balaram, P. *Proc. Natl. Acad. Sci. U.S.A.* **2000**, *97*, 3034–3037. (e) McDonnell, K. A.; Imperiali, B. *J. Am. Chem. Soc.* **2001**, *123*, 1002–1003. (f) Bolon, D. L.; Mayo, S. L. *Proc. Natl. Acad. Sci. U.S.A.* **2001**, *98*, 14274–14279. (g) Xing, G.; DeRose, V. J. *Curr. Opin. Chem. Biol.* **2001**, *5*, 196–200. (h) Di Constanzo, L.; Wade, H.; Geremia, S.; Randaccio, L.; Pavone, V.; DeGrado, W. F.; Lombardi, A. *J. Am. Chem. Soc.* **2001**, *123*, 12794–12757. (i) Benson, D. E.; Haddy, A. E.; Hellinga, H. W. *Biochemistry* **2002**, *41*, 3262–3269. (j) Wey, Y.; Hecht, M. H. *Protein Eng. Des.* **2004**, *17*, 67–75. (k) Gibney, B. R.; Rabanal, F.; Skalicky, J. J.; Wand, A. J.; Dutton, P. L. *J. Am. Chem. Soc.* **1997**, *119*, 2323–2324. (l) Reedy, C. J.; Gibney, B. R. *Chem. Rev.* **2004**, *104*, 617–649.

(5) (a) Moffet, D. A.; Hecht, M. H. *Chem. Rev.* **2001**, *101*, 3191–3203. (b) Bolon, D. N.; Voigt, C. A.; Mayo, S. L. *Curr. Opin. Chem. Biol.* **2002**, *6*, 125–132. (c) Socolich, M.; Lockless, S. W.; Russ, W. P.; Lee, H.; Gardner, K. H.; Ranganathan, R. *Nature* **2005**, *437*, 512–518. (d) Bradley, P.; Misura, K. M.; Baker, D. *Science* **2005**, *309*, 1868–1871. (e) Wunderlich, M.; Martin, A.; Staab, C. A.; Schmid, F. X. *J. Mol. Biol.* **2005**, *351*, 1160–1168.

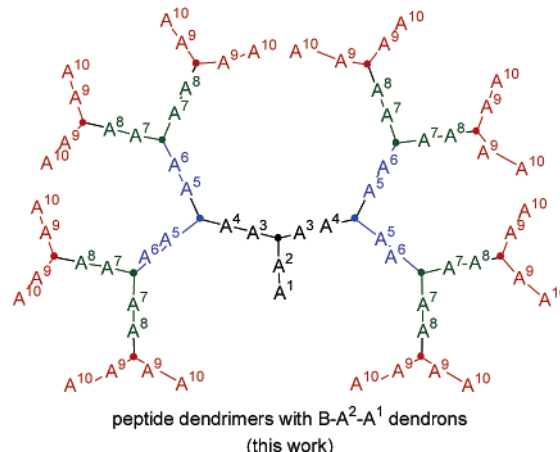
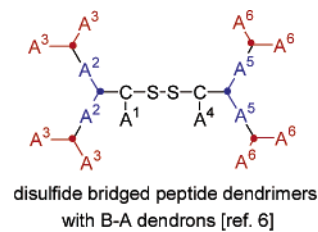


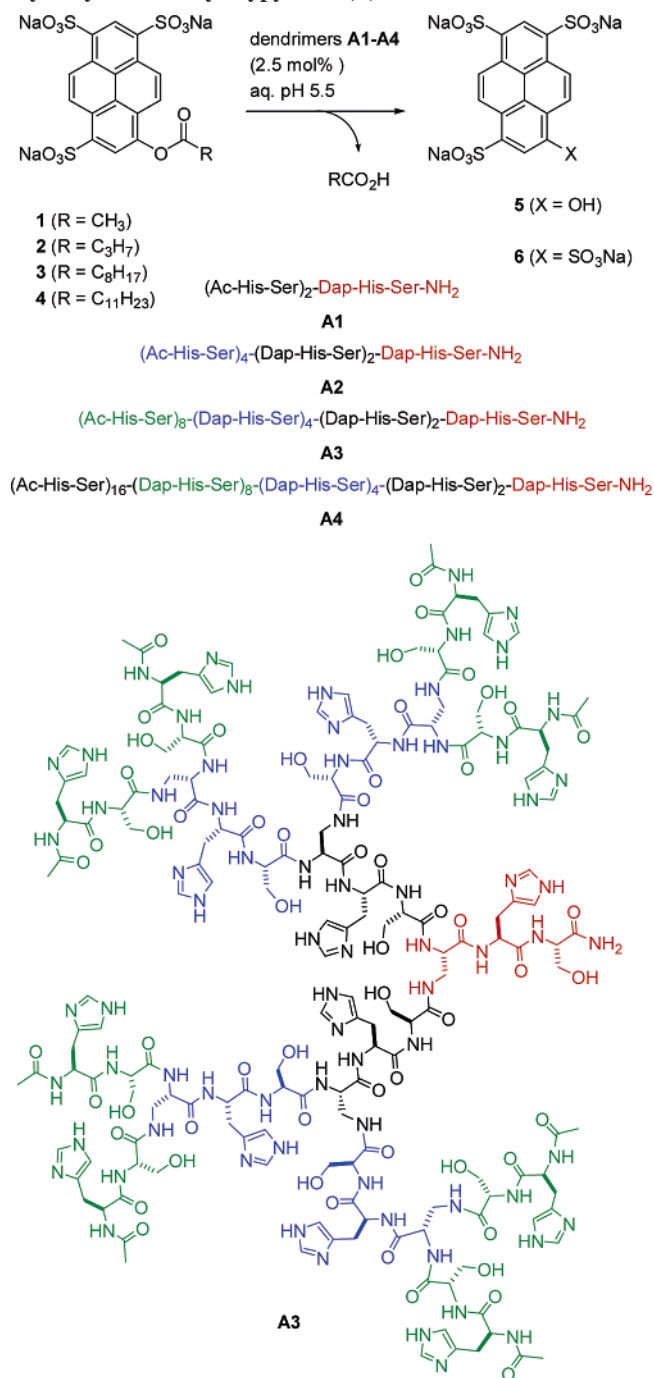
**FIGURE 1.** Architectures of peptide dendrimers. The variable amino acids A<sup>n</sup> are branched by using diamino acids B (● in the drawing) such as L-2,3-diamino propionic acid (Dap). The peptide dendrimers are synthesized by Fmoc-solid-phase peptide synthesis.

We prepared dendritic peptides by alternating proteinogenic  $\alpha$ -amino acids (A<sup>n</sup>) with a branching diamino acid (B) to form second generation dendrimers of type A<sub>4</sub>(BA<sup>2</sup>)B-Cys-A<sup>1</sup>, which were then dimerized by disulfide bond formation to obtain third generation dendrimers (Figure 1). Dendrimers displaying multiple histidine residues on their surface catalyzed the hydrolysis of fluorogenic esters in aqueous media with enzyme-like properties of substrate binding and multiple catalytic turnover.<sup>6</sup>

The convergent strategy by disulfide bond formation used in these initial studies proved relatively cumbersome since it required purification of the intermediate half-dendrimers before dimerization. The dendrimer topology was therefore modified to allow for a complete synthesis on solid support and a single purification. Peptide dendrimers were prepared with two variable amino acid positions per branch, corresponding to a dendron of type B-A<sup>2</sup>-A<sup>1</sup>, allowing a similar number of variable amino acid positions per dendrimer (Figure 1). In a preliminary study, the peptide dendrimers **A1–A4** were prepared with a repeating Dap-His-Ser dendron (Dap = L-2,3-diaminopropionic acid). These dendrimers exhibited esterase-type catalytic activity, and a strong positive dendritic effect was observed for the hydrolysis of 8-acyloxy-1,3,6-pyrene trisulfonates **1–3** (Scheme 1).<sup>7</sup> Herein we report a synthetic and mechanistic study of 32 different dendrimer mutants in this series, which establishes the robustness of the peptide dendrimer synthesis and catalytic properties observed. An automated parallel synthesis protocol was devel-

(6) (a) Esposito, A.; Delort, E.; Lagnoux, D.; Djojo, F.; Reymond, J.-L. *Angew. Chem., Int. Ed.* **2003**, *42*, 1381–1383. (b) Lagnoux, D.; Delort, E.; Douat-Casassus, C.; Esposito, A.; Reymond, J. L. *Chem. Eur. J.* **2004**, *10*, 1215–1226. (c) Douat-Casassus, C.; Darbre, T.; Reymond, J.-L. *J. Am. Chem. Soc.* **2004**, *126*, 7817–7826.

(7) Delort, E.; Darbre, T.; Reymond, J.-L. *J. Am. Chem. Soc.* **2004**, *126*, 15642–15643.

**SCHEME 1. Peptide Dendrimers A1–4 Catalyze the Hydrolysis of 8-Acyloxy pyrene 1,3,6-Trisulfonates 1–3<sup>a</sup>**


<sup>a</sup> Dap = L-2,3-diaminopropionic acid. His = L-histidine. Ser = L-serine.

oped to facilitate the synthesis of analogues. The influence of amino acid composition, dendrimer size, and amino acid side chain ionization state on substrate binding and catalytic efficiency was determined.

## Results and Discussion

**Initial Studies.** Dendrimers **A1–A4** built by iteration of the diamino acid dendron Dap-His-Ser were obtained in good yields and high purity by sequential coupling of Fmoc-protected amino acid building block by standard solid-supported peptide synthesis

(Scheme 2).<sup>8</sup> Dendrimers **A1–A4** were obtained by using a tentagel-type resin with a loading of 0.25 mmol/g. The fourth generation dendrimer **A4** was obtained in only moderate yields, suggesting an upper limit for synthesis (see Table 2 below). Indeed an attempted synthesis of a fifth generation dendrimer was unsuccessful.

Investigation of the catalytic properties of dendrimers **A1–A4** revealed an unusually strong positive dendritic effect for the hydrolysis of pyrene trisulfonate esters **1–3** in aqueous media, with both the catalytic rate constant  $k_{\text{cat}}$  and substrate binding  $1/K_M$  increasing with dendrimer size, resulting in a quadratic increase in the specificity constants  $k_{\text{cat}}/K_M$  (Figure 2).

The proportionality of the catalytic rate constant  $k_{\text{cat}}$  to the total number of histidine residues in dendrimers **A1–A4** suggested a direct role for this residue in catalysis, which should be visible in a pH–rate profile analysis. The pH profile for hydrolysis of butyrate ester **3** was determined for dendrimers **A3** and **A4** and the reference catalyst 4-methylimidazole (4-MeIm), a model for the histidine side chain. The pH–rate profile for catalysis of 4-MeIm showed a pH-dependent increase in the range studied. On the other hand, the pH–rate profile of  $k_{\text{cat}}$  with the dendrimers was very different, showing a rather flat pH dependence with a maximum activity around pH 5.5.<sup>7</sup>

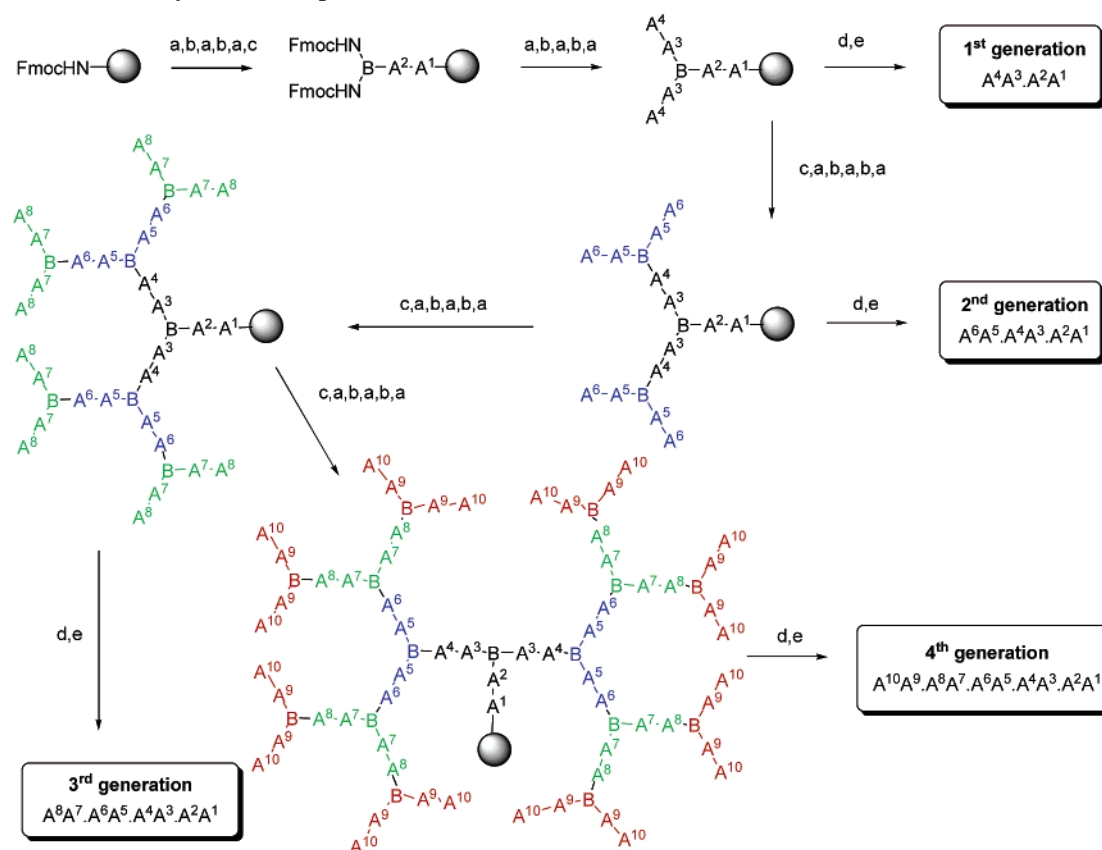
The pH–rate profile of 4-MeIm was consistent with the free base form of 4MeIm acting either as nucleophile or as general base catalyst, as has been proposed in similar studies of histidine containing artificial enzymes.<sup>9</sup> The relatively flat pH–rate profile of the peptide dendrimers, by contrast, suggested that both protonated and free base histidine residues might act in concert in the dendrimer-catalyzed reaction. The free base form of histidine could act as a nucleophilic or general base catalyst promoting nucleophilic addition to the ester carbonyl group, while another protonated histidine side chain might help stabilize the oxyanion intermediate (Scheme 3). Since the rate constant  $k_{\text{cat}}$  measures the reaction of bound substrate to bound transition state, the stabilizing effect of the protonated histidine would be expected in addition to a possible contribution to substrate binding (see below). A similar bifunctional mechanism has been suggested by other authors for similar ester hydrolysis reactions catalyzed by imidazole containing systems.<sup>10</sup>

The concerted action of histidine side chains in such a mechanism should depend on the precise relative positioning of at least two such side chains within the dendrimer. Such a requirement for a precise relative positioning of catalytic groups could imply that relatively small structural changes within the dendrimers might lead to significant changes in catalytic

(8) (a) Lloyd-Williams, P.; Albericio, F.; Giralt, E. *Chemical Approaches to the Synthesis of Peptides and Proteins*; CRC Press: Boca Raton, FL, 1997. (b) Chan, C.; White, P. D. *Fmoc Solid-Phase Peptide Synthesis: a practical approach*; Oxford Press: New York, 2000.

(9) Nilsson, J.; Baltzer, L. *Chem. Eur. J.* **2000**, *6*, 2214–2220.

(10) (a) Broo, K. S.; Brive, L.; Ahlberg, P.; Baltzer, L. *J. Am. Chem. Soc.* **1997**, *119*, 11362–11372. (b) Broo, K. S.; Nilsson, H.; Nilsson, J.; Flodberg, A.; Baltzer, L. *J. Am. Chem. Soc.* **1993**, *115*, 4063–4068. (c) Broo, K. S.; Nilsson, H.; Nilsson, J.; Baltzer, L. *J. Am. Chem. Soc.* **1998**, *120*, 10287–10295. (d) Baltzer, L.; Kerstin, S. B.; Nilsson, H.; Nilsson, J. *Bioorg. Med. Chem.* **1999**, *7*, 83–91. (e) Klotz, I. M. *Adv. Chem. Phys.* **1978**, *39*, 109–176. (f) Nango, M.; Klotz, I. M. *J. Polym. Sci., Polym. Chem. Ed.* **1978**, *16*, 1265–1273. (g) Overberger, C. G.; Salomone, J. C. *Acc. Chem. Res.* **1969**, *2*, 217–224. (h) Overberger, C. G.; Kawakami, Y. *J. Polym. Sci.: Polym. Chem. Ed.* **1978**, *16*, 1237–1248. (i) Tomko, R.; Overberger, C. G. *J. Polym. Sci.: Polym. Chem. Ed.* **1985**, *23*, 265–277. (j) Breslow, R.; Schmuck, C. *J. Am. Chem. Soc.* **1996**, *118*, 6601–6605. (k) Baumeister, B.; Sakai, N.; Matile, S. *Org. Lett.* **2001**, *3*, 4229–4332. (l) Som, A.; Matile, S. *Eur. J. Org. Chem.* **2002**, 3874–3883.

SCHEME 2. Solid Phase Synthesis of Peptide Dendrimers<sup>a</sup>

<sup>a</sup> A<sup>n</sup> = variable amino acid. B = Dap (2,3-diaminopropionic acid). Conditions: (a) DMF/piperidine (4:1), 2 × 10 min; (b) Fmoc-A<sup>n</sup>-OH, BOP/DIEA; (c) (Fmoc)<sub>2</sub>Dap, BOP/DIEA; (d) Ac<sub>2</sub>O/DCM (1:1), 1 h; (e) TFA/TIS/H<sub>2</sub>O (94/5/1), 4 h, then preparative HPLC purification.

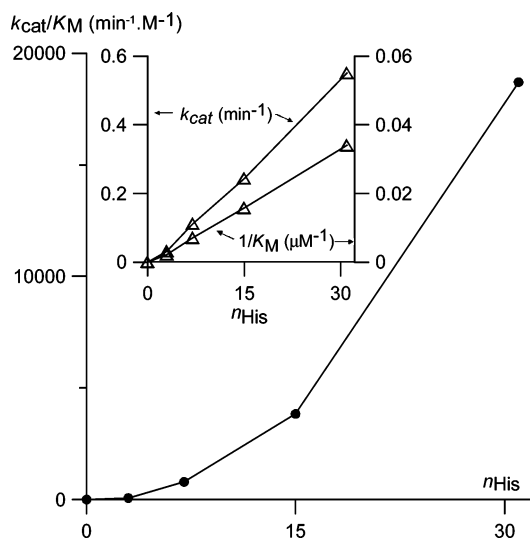


**FIGURE 2.** Dendritic effect on dendrimer-catalyzed hydrolysis of butyrate **2** for **A1** to **A4**. Conditions: 10–1000 μM substrate, **A1** = 10.6 μM, **A2** = 6.4 μM, **A3** = 3.55 μM, **A4** = 1.88 μM in aqueous 5 mM citrate pH 5.5, 26 °C.  $n_{\text{His}}$  gives the total number of histidine residues in the dendrimer. Similar plots were obtained on substrates **1** and **3**.

efficiency, suggesting that a mutational study might uncover more active dendrimers.

The proportionality of substrate binding  $1/K_M$  to dendrimer size, participating in the positive dendritic effect observed

(Figure 2), was traced back to increased binding to the acyl chain of the substrates in higher generation dendrimers. Thus, isothermal calorimetry (ITC) measurements with dendrimers **A1**–**A4** and the nonreactive substrate **4**<sup>11</sup> or the reaction product **5** showed that the number of binding sites per dendrimer increased with generation number for both **4** and **5**, with an average of one substrate or product binding site per three histidine residues (Table 1). A dendritic effect on binding affinity was observed with substrate **4** following the trend in  $K_M$  observed with the reactive substrates **1**–**3**. By contrast the binding constant for product **5**, which was 10-fold weaker than that of the substrate, remained constant from **A1** to **A4**. Binding with both **4** and **5** was driven by a large and favorable enthalpy ( $\Delta H_a$  values between –7 and 11.6 kcal/mol) with favorable contribution of  $\Delta S$  that could be attributed to solvent release upon binding.<sup>12</sup> The strong binding between the higher generation dendrimer **A4** and the longest acyl-chain substrates could be interpreted in terms of hydrophobic interactions between the substrate's acyl chain and the dendrimer interior. Such hydrophobic interactions are also consistent with the fact that the  $K_M$  values for the more hydrophobic nonanoate ester **3** are generally lower than those for the corresponding butyrate **2** or acetate **1** across the dendrimer series.

(11) Dodecanoyl ester **4** gave very low conversion and competitively inhibited catalysis for the shorter chain substrates, making this substrate an ideal model for studying substrate binding to the dendrimers.

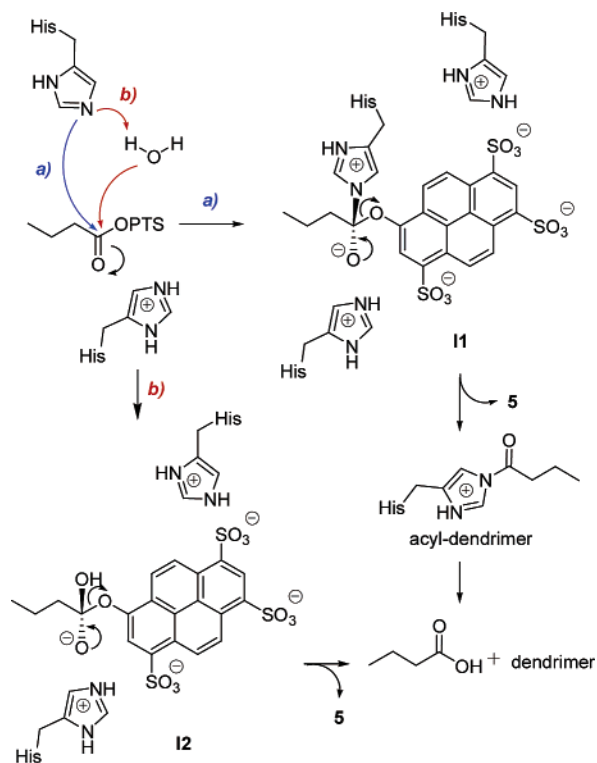
(12) (a) Zechel, D. L.; Boraston, A. B.; Gloster, T.; Boraston, C. M.; Macdonald, J. M.; Tilbrook, D. M. G.; Stick, R. V.; Davies, G. J. *J. Am. Chem. Soc.* **2003**, *125*, 14313–14323. (b) Rekharsky, M.; Inoue Y.; Tobey, S.; Metzger, A.; Anslyn, E. *J. Am. Chem. Soc.* **2002**, *124*, 14959–14967.

**TABLE 1.** Calorimetric Titration of Nonreactive Substrate **4** and the Reaction Product **5** Added to **A1–A4**: Thermodynamic Parameters, Association Constants ( $K_a$ ), Number of Binding Sites ( $n$ )<sup>a</sup>

	$N_{\text{His}}$	$n$	$K_a$ ( $\times 10^4 \text{ M}^{-1}$ )	$\Delta H_a$ (kcal/mol)	$\Delta G_a$ (kcal/mol)	$\Delta S_a$ (cal/mol/K)	
<b>A1</b>	5	3	0.84( $\pm 0.22$ )	0.11( $\pm 0.02$ )	-8.36( $\pm 2.46$ )	-17.47( $\pm 0.45$ )	31( $\pm 10$ )
<b>A2</b>	5	7	1.69( $\pm 0.09$ )	0.27( $\pm 0.03$ )	-7.74( $\pm 0.59$ )	-19.67( $\pm 0.28$ )	40( $\pm 3$ )
<b>A3</b>	5	15	4.78( $\pm 0.43$ )	0.29( $\pm 0.05$ )	-8.89( $\pm 1.07$ )	-19.91( $\pm 0.43$ )	37( $\pm 5$ )
<b>A4</b>	5	31	9.43( $\pm 1.5$ )	0.28( $\pm 0.07$ )	-10.06( $\pm 1.92$ )	-19.76( $\pm 0.62$ )	32( $\pm 8$ )
<b>A1</b>	4	3	2.36( $\pm 0.07$ )	1.66( $\pm 0.51$ )	-6.91( $\pm 0.33$ )	-24.20( $\pm 0.77$ )	58( $\pm 4$ )
<b>A2</b>	4	7	1.86( $\pm 0.04$ )	10.5( $\pm 3.2$ )	-12.85( $\pm 0.38$ )	-28.79( $\pm 0.76$ )	53( $\pm 4$ )
<b>A3</b>	4	15	5.83( $\pm 0.03$ )	56.2( $\pm 12.0$ )	-10.85( $\pm 0.11$ )	-32.98( $\pm 0.53$ )	74( $\pm 2$ )
<b>A4</b>	4	31	9.88( $\pm 0.04$ )	80.8( $\pm 15.0$ )	-11.58( $\pm 0.10$ )	-33.87( $\pm 0.46$ )	74( $\pm 2$ )

<sup>a</sup> Conditions: **A1** 0.5 mM, **A2** 0.2 mM, **A3** 0.1 mM, **A4** 0.05 mM, **4** 10 mM, **5** 10 mM in citrate buffer pH 5.5 (5 mM), at 27 °C.

### SCHEME 3. Mechanistic Proposal for Dendrimer Catalyzed Ester Hydrolysis<sup>a</sup>



<sup>a</sup> Reaction processes: (a) nucleophilic attack of histidine generated an acyl-dendrimer intermediate; (b) general base catalyzed nucleophilic attack of a water molecule

**Synthesis of Hydrophobic Core Dendrimers.** A series of analogue dendrimers were prepared to investigate the effect of amino acid substitutions on substrate binding and catalytic efficiency. The introduction of hydrophobic residues at the dendrimer core together with catalytic and charged amino acids at the surface was first investigated with the aim of creating more protein-like dendrimers. Indeed, natural protein folding is driven by the hydrophobic collapse,<sup>13</sup> which results in an aggregation of apolar residues at the protein core, while polar and charged residues are found near the surface. Similarly, peptide dendrimers with a hydrophobic core and polar residues

on the surface might provide interesting mimics of proteins.<sup>14</sup> Hydrophobic core dendrimers might also allow enhanced hydrophobic interactions with the substrates similar to those observed by ITC with **A1–A4** (Table 1).

We prepared a direct analogue series **B1–B3** featuring a phenylalanine-leucine at the core and the serine-histidine dyad in the branches. An attempted synthesis of the fourth generation dendrimer **B4** was unsuccessful. In addition we also prepared a diverse set of dendrimers **C1–O4** incorporating negatively charged and hydrophobic residues, which might reduce the selectivity of the dendrimers for anionic substrates. The syntheses were carried out with Tentagel or Rink amide resin, and the dendrimers were isolated in pure form with satisfactory yields. In the case of dendrimer **G2**, some dimerization took place by air oxidation, and part of the dendrimer was isolated as the disulfide bridged homodimer **G22** (Table 2).

The catalytic properties of the 17 dendrimers **B1–O4** were investigated together with **A1–A4**. A survey of various ester substrates showed that the substrate scope of these histidine containing dendrimers was limited to 8-acyloxy-1,3,6-pyrene trisulfonates. There was no significant catalysis by any of the dendrimers for the hydrolysis of cationic substrate **7**, neutral substrates **8** and **9a–c**, or the more hydrophobic fluorescein substrates **10a–c** (Figure 3).<sup>15</sup>

The peptide dendrimer series **B1–O4** was compared with **A1–A4** for hydrolysis of the 8-acyloxy-1,3,6-pyrene trisulfonates **1–4** in aqueous buffer pH 6.0. The apparent catalytic effect in the analogue series **B1–O4** was much weaker than that with the histidine-serine series **A1–A4**. Dendrimer **G22** formed by spontaneous oxidative dimerization of **G2** during purification also did not show strong catalysis. Dendrimers **B1–B3** bearing the leucine-phenylalanine hydrophobic core showed acceptable catalytic properties with substrates **1–3**, and were studied in detail (see below). The generally low activity of this dendrimer series incorporating hydrophobic core residues suggested that a different strategy should be followed to improve catalysis.

**Parallel Synthesis of Analogues of Dendrimer A3.** Peptide dendrimer **A3** gave the best compromise between an acceptable chemical yield by synthesis and a strong catalytic activity. Due to the low activity of the dendrimer analogues incorporating hydrophobic residues discussed above, we turned our attention to conservative replacements of serines with similarly small and polar residues such as alanine (**A3A**),  $\beta$ -alanine (**A3B**), or threonine (**A3C**) as a strategy to optimize catalytic activity. We

(13) (a) Gerstman, B. S.; Chapagain, P. P. *J. Chem. Phys.* **2005**, *123*, 054901/1–054901/6. (b) Zhou, R.; Huang, X.; Margulis, C. J.; Berne, B. *J. Science* **2004**, *305*, 1605–16. (c) Tanford, C. *The Hydrophobic Effect*, 2nd ed.; Wiley-Interscience, New York, 1980. (d) Pratt, L. R.; Pohorille, A. *Chem. Rev.* **2002**, *102*, 2671–2691. (e) Schneider, J. P.; Kelly, J. W. *Chem. Rev.* **1995**, *95*, 2169–2187. (f) Breslow, R.; Yang, Z.; Ching, R.; Trojandt, G.; Odobel, F. *J. Am. Chem. Soc.* **1998**, *120*, 3536–3537.

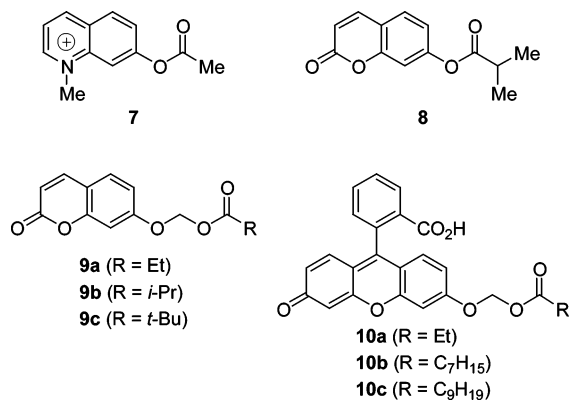
(14) Clouet, A.; Darbre, T.; Reymond, J.-L. *Adv. Synth. Catal.* **2004**, *346*, 1195–1204.

(15) (a) Bensel, N.; Reymond, M. T.; Reymond, J.-L. *Chem. Eur. J.* **2001**, *7*, 4604–4612. (b) Leroy, E.; Bensel, N.; Reymond, J.-L. *Bioorg. Med. Chem. Lett.* **2003**, *13*, 2105–2108.

**TABLE 2.** Peptide Dendrimer Series A–O of Different Generation Number Containing Histidine as the Catalytic Residue, with Yields after Preparative HPLC, Calculated Molecular Weight, and Their Mass Obtained by Electron Spray MS (positive mode), and Their Apparent Catalytic Effect  $V_{\text{net}}/V_{\text{un}}^a$ 

no.	sequence $A^n A^{n-1} \dots A^4 A^3 \dots A^2 A^1$	resin loading (mmol/g)	$m$ (mg)	yield (%)	MW	MS (ES+)	$V_{\text{net}}/V_{\text{un}}$		
							1	2	3
A1	HS.HS	0.25 <sup>c</sup>	3.3	11	859.37	859.38	3.3	4.6	3.3
A2	HS.HS.HS	0.25 <sup>c</sup>	21.9	31	2011.85	2012.25	30	38	26
A3	HS.HS.HS.HS	0.25 <sup>c</sup>	34.2	23	4316.81	4318.13	90	110	60
A4	HS.HS.HS.HS.HS	0.25 <sup>c</sup>	10.4	3.3	8926.73	8929.25	170	180	160
B1	HS.LF	0.18 <sup>c</sup>	19.7	49	895.43	895.50	6.8	7.0	1.3
B2	HS.HS.LF	0.18 <sup>c</sup>	31.2	63	2047.91	2048.50	13	9.8	0.5
B3	HS.HS.HS.LF	0.18 <sup>c</sup>	8.6	16	4352.87	4353.13	26	10	0.3
C1	HD.CS	0.61 <sup>b</sup>	4.3	13	881.31	881.75	0.3	0.4	0.4
D2	DH.HS.CF	0.47 <sup>b</sup>	11.1	24	2149.82	2150.00	3.0	5.5	4.2
E2	HD.SF.CL	0.61 <sup>b</sup>	11.1	14	2135.85	2136.75	0.6	0.2	0.3
F2	HS.DF.CL	0.61 <sup>b</sup>	4.6	5.9	2079.86	2080.63	1.7	2.8	1.9
G2	HDS.HD.CS	0.61 <sup>b</sup>	3.8	3.9 <sup>d</sup>	2493.90	2494.25	0.3	0.0	0.0
G22	(HDS.HD.CS) <sub>2</sub>	0.61 <sup>b</sup>	1.6	1.6 <sup>d</sup>	4985.78	4987.88	0.1	0.0	0.2
H2	HS.DF.AL	0.20 <sup>c</sup>	8.5	34	2047.89	2048.50	0.2	0.7	1.1
I2	HS.AF.AL	0.18 <sup>c</sup>	12.7	29	1959.91	1960.38	3.6	5.7	8.2
J2	HA.AF.AL	0.29 <sup>c</sup>	18.2	13	1895.93	1896.50	3.4	4.4	6.5
K2	HA.DF.AL	0.43 <sup>b</sup>	31.3	30	1983.91	1984.63	1.4	2.6	3.6
L3	DS.SH.FL.CF	0.20 <sup>c</sup>	16.1	17	4238.67	4240.25	0.4	0.0	0.0
M3	DH.HS.DF.AL	0.20 <sup>c</sup>	26.7	45	4576.81	4578.13	1.7	3.2	7.3
N3	DH.HA.DF.AL	0.43 <sup>b</sup>	34.6	32	4512.83	4513.63	2.5	4.5	4.5
O4	HS.DH.HA.DF.AL	0.43 <sup>b</sup>	4.6	3.5	9120.77	9123.75	42	68	44

<sup>a</sup> Conditions: 200  $\mu\text{M}$  substrate **1**, **2**, **3**, dendrimers 5  $\mu\text{M}$ , in 20 mM Bis Tris buffer pH 6.0.  $V_{\text{un}}$  = rate in buffer alone with 200  $\mu\text{M}$  substrate;  $V_{\text{net}} = V_{\text{cat}} - V_{\text{un}}$ ,  $V_{\text{cat}}$  = apparent rate in the presence of 2.5 mol % dendrimer catalyst and 200  $\mu\text{M}$  substrate. There was no catalysis with substrate **4** and any of these dendrimers. <sup>b</sup> Rink amide resin. <sup>c</sup> NovaSyn TGR resin. <sup>d</sup> Isolated from the same reaction, total yield = 5.5%.

**FIGURE 3.** Fluorogenic substrates tested for peptide dendrimer catalyzed ester hydrolysis.

also systematically exchanged histidine residues against alanine at the inner or outer branches until complete removal to clarify their role in substrate binding and catalysis (**A3D**–**A3J**). Finally histidine was either used at every position (**A3K**) or the amino acids were reshuffled between the different positions (**A3L**–**A3O**) to investigate the effect of amino acid positions on catalysis.

A parallel synthesis protocol was developed to demonstrate the feasibility of automated dendrimer synthesis. The synthesizer uses solutions of reagents at fixed concentrations rather than adding solids into the reactor as during manual synthesis. This different addition mode implies that coupling reactions require increasing volume as the synthesis proceeds to higher generations of the dendrimer. The synthesis was carried out with tentagel resin (0.23 mmol/g), following the synthetic route for third generation dendrimers (Scheme 2). Coupling times were 1 h for the first generation, 2 h for the second generation, and 4 h for the third generation, using systematic double coupling. The coupling reagent was HBTU/HOBt (0.5 M in DMF, 3

equiv) with *N*-methylmorpholine as base (5 equiv).<sup>16</sup> Cleavage and purification of the peptides were then carried out manually. The quality of the crude products and the isolated yields after purification by preparative HPLC were comparable to those obtained by manual synthesis (see the Supporting Information).

**Catalytic Properties of B1–B3 and A3-Analogue Series.** The hydrophobic core series **B1**–**B3** and 15 analogues of the histidine-serine dendrimer **A3** obtained by parallel synthesis were characterized in detail. As for the hydrophobic core series discussed above, catalytic activity was found to be specific for 8-acyloxy-1,3,6-pyrene trisulfonates, with no detectable catalysis with other types of substrates (Figure 3). The dendrimers were therefore investigated for their catalytic properties in the hydrolysis of the fluorogenic ester substrates **1**–**4**.

All assays were conducted in aqueous citrate buffer at pH 5.5, which are optimal conditions for this system,<sup>7</sup> and the reactions were followed by fluorescence in a microtiter plate reader. Rate enhancement was first assessed by the value of the apparent catalytic effect  $V_{\text{net}}/V_{\text{un}}$  measured at 200  $\mu\text{M}$  substrate and 1.8 mol % catalyst (Table 3).

Catalysis as judged by  $V_{\text{net}}/V_{\text{un}}$  depended mostly on the total number of histidine residues in the dendrimer ( $N_{\text{His}}$ ), in agreement with the role of histidine as a catalytic residue. Thus the control dendrimer **A3J** without histidine and its analogue **A3I** with only one histidine residue at the core were catalytically inactive. On the other hand all dendrimers with 15 or more histidines were strongly active, although structural variations caused large differences in apparent activity. Five dendrimers were much more active than the reference catalyst **A3**. These were the **A3** mutants serine  $\rightarrow$  alanine **A3A**, serine  $\rightarrow$   $\beta$ -alanine **A3B**, and serine  $\rightarrow$  threonine **A3C**, dendrimer **A3L** with 24 histidines in the outer layers and 6 serines in the inner layers, and its analogue **A3M** with alternating histidine and serine generations. By contrast, the whole-histidine dendrimer **A3K**

(16) Carpino, L. A.; El-Faham, A. *J. Org. Chem.* **1994**, *59*, 695–697.

TABLE 3. Analogues A3A–A3O of Dendrimers A3 Prepared Par Automated Synthesis on the Chemspeed PSW1100 Peptide Synthesizer<sup>a</sup>

sequence	$N_{\text{His}}$	$m$ (mg)	yield (%)	MW	MS (ES+)	$V_{\text{net}}/V_{\text{un}}$			
						1	2	3	
A3	HS.HS.HS.HS	15	7.0	5.0	4316.81	4318.13	161	242	105
A3A	HA.HA.HA.HA	15	7.8	5.9	4076.89	4078.00	160	370	140
A3B	H $\beta$ A.H $\beta$ A.H $\beta$ A.H $\beta$ A	15	17.2	12.9	4076.89	4079.13	300	1100	580
A3C	HT.HT.HT.HT	15	19.1	13.3	4525.05	4528.75	260	850	280
A3D	HS.AS.AS.AS	8	19.0	17.3	3854.66	3855.88	33	100	57
A3E	AS.HS.HS.HS	7	15.8	15.0	3788.64	3789.63	77	140	81
A3F	AS.HS.HS.HA	7	2.0	1.9	3772.64	3773.38	48	115	53
A3G	AS.HS.HS.AS	6	10.3	10.2	3722.62	3723.88	67	170	37
A3H	AS.HS.AS.AS	4	5.8	6.2	3590.57	3591.5	16	33	7
A3I	AS.AS.AS.HS	1	7.9	9.8	3392.51	3393.88	0	0	1.8
A3J	AS.AS.AS.AS	0	14	18.3	3326.48	3327.5	1	1.5	0.9
A3K	HH.HH.HH.HH	30	2.0	1.0	5067.21	5068.75	36	64	17
A3L	HH.HH.SS.SS	24	23	13.3	4767.05	4768.63	280	1100	280
A3M	HH.SS.HH.SS	20	7.4	4.7	4566.95	4568.63	250	760	560
A3N	AH.AH.AH.AH	15	13.8	10.4	4076.89	4079.13	154	390	330
A3O	SH.SA.SH.SA	10	20.7	17.6	3986.7	3988.13	90	190	74

<sup>a</sup> Given yields after preparative HPLC. Mass obtained by electron spray MS (positive mode). Apparent catalytic effect  $V_{\text{net}}/V_{\text{un}}$ . Conditions: 200  $\mu\text{M}$  substrate **1**, **2**, **3**, dendrimers 3.55  $\mu\text{M}$  (1.8 mol %), in 5 mM citrate buffer pH 5.5. There was no catalysis with substrate **4** and any of these dendrimers.

TABLE 4. Michaelis–Menten Parameters on Pyrene Substrates **1**, **2**, and **3**<sup>a</sup>

dendrimer	sequence	$N_{\text{His}}$	$K_{\text{M}}$ (mM)			$k_{\text{cat}}/k_{\text{uncat}}^b$			$((k_{\text{cat}}/K_{\text{M}})/k_2)^c$		
			1	2	3	1	2	3	1	2	3
A1	HS.HS	3	0.840	0.450	1.60	1800	2300	4500	140	140	130
A2	HS.HS.HS	7	0.110	0.140	0.067	3600	8000	4400	2000	1600	3000
A3	HS.HS.HS.HS	15	0.041	0.063	0.013	6800	17000	6700	10000	7900	23000
A4	HS.HS.HS.HS.HS	31	0.035	0.029	0.006	20000	40000	18000	35000	38000	140000
B1	HS.LF	2	1.891	0.537	0.936	1353	1126	1322	45	60	65
B2	HS.HS.LF	6	0.610	0.126	0.064	4847	3616	1978	501	821	1420
B3	HS.HS.HS.LF	14	0.158	0.083	0.010	2990	5400	1780	1190	1872	8198
A3A	HA.HA.HA.HA	15	0.070	0.060	0.025	11000	23000	8200	9200	10500	1500
A3B	H $\beta$ A.H $\beta$ A.H $\beta$ A.H $\beta$ A	15	0.050	0.070	0.030	21000	80000	34000	28000	34000	54000
A3C	HT.HT.HT.HT	15	0.100	0.160	0.040	22000	90000	16000	13000	15000	20000
A3D	HS.AS.AS.AS	8	0.650	0.240	0.240	8000	9500	6700	760	1100	1300
A3E	AS.HS.HS.HS	7	0.640	1.100	0.210	15000	52000	9900	1500	1400	2100
A3F	AS.HS.HS.HA	7	0.250	0.200	0.150	5600	11000	5900	1400	1500	1800
A3G	AS.HS.HS.AS	6	0.230	0.310	0.120	7700	19000	3900	2100	18000	1500
A3H	AS.HS.AS.AS	4	0.420	0.740	<i>d</i>	3000	9400	<i>d</i>	440	360	<i>d</i>
A3I	AS.AS.AS.HS	1	<i>d</i>	<i>d</i>	<i>d</i>	<i>d</i>	<i>d</i>	<i>d</i>	<i>d</i>	<i>d</i>	<i>d</i>
A3J	AS.AS.AS.AS	0	<i>d</i>	<i>d</i>	<i>d</i>	<i>d</i>	<i>d</i>	<i>d</i>	<i>d</i>	<i>d</i>	<i>d</i>
A3K	HH.HH.HH.HH	30	0.050	0.020	<i>d</i>	2600	3900	<i>d</i>	3280	4800	<i>d</i>
A3L	HH.HH.SS.SS	24	0.080	0.080	0.008	23000	80000	17000	18500	28000	91000
A3M	HH.SS.HH.SS	20	0.080	0.090	0.050	18000	10000	25000	13800	3000	25000
A3N	AH.AH.AH.AH	15	0.080	0.070	0.050	11000	26000	22000	8800	11000	19000
A3O	SH.SA.SH.SA	10	0.260	0.910	0.100	9800	72000	7600	2300	2200	3400

<sup>a</sup> Conditions: 10–1000  $\mu\text{M}$  substrate, dendrimer concentration 3.55  $\mu\text{M}$  for **A3** and **A3A–A3O**, 10.6  $\mu\text{M}$  for **A1**, 6.4  $\mu\text{M}$  for **A2**, 1.88  $\mu\text{M}$  for **A4**, 16  $\mu\text{M}$  for **B1**, 8  $\mu\text{M}$  for **B2**, 4  $\mu\text{M}$  for **B3**, in aq 5 mM citrate pH 5.5, 26°C. <sup>b</sup>  $k_{\text{uncat}} = 4.39 \times 10^{-5} \text{ min}^{-1}$  for **1**,  $1.39 \times 10^{-5} \text{ min}^{-1}$  for **2**, and  $2.20 \times 10^{-5} \text{ min}^{-1}$  for **3**. <sup>c</sup>  $k_2 = 4\text{-MeIm} = 6.96 \times 10^{-4} \text{ mM}^{-1} \text{ min}^{-1}$  for **1**,  $4.86 \times 10^{-4} \text{ mM}^{-1} \text{ min}^{-1}$  for **2**, and  $4.77 \times 10^{-4} \text{ mM}^{-1} \text{ min}^{-1}$  for **3**. <sup>d</sup> No activity detected.

was much less active than **A3**, showing that the number of histidines alone was not sufficient to explain the apparent catalytic rate. By comparison the hydrophobic core dendrimers **B1–B3** with the phenylalanine-leucine dyad at positions A<sup>2</sup>A<sup>1</sup> were much less catalytically active.

Michaelis–Menten parameters were determined for the different dendrimers with substrates **1–3** (Table 4). The rate accelerations  $k_{\text{cat}}/k_{\text{uncat}}$  ranged from  $10^2$  to  $10^5$ , with the highest value of  $k_{\text{cat}}/k_{\text{uncat}} = 90\,000$  being observed for the histidine-threonine dendrimer **A3C** with the butyrate ester **2**. Substrate binding varied between  $K_{\text{M}} = 8 \mu\text{M}$  for dendrimer **A3L** and nonanoate **3**, and  $K_{\text{M}} = 1100 \mu\text{M}$  for dendrimer **A3E** with butyrate **2**.

**Kinetic Profiling and Clustering.** The series **A1–A4** showed a linear correlation between the total number of histidine residues ( $N_{\text{His}}$ ) and the catalytic parameters  $k_{\text{cat}}$  and  $1/K_{\text{M}}$ ,

suggesting that this residue was responsible for both catalysis and binding (Figure 2). To test whether this relationship held true throughout the dendrimer series, the influence of  $N_{\text{His}}$  on catalytic parameters was analyzed by multivariate statistical analysis.<sup>17</sup> Each dendrimer was described by seven variables defined as the catalytic parameters  $k_{\text{cat}}$  and  $1/K_{\text{M}}$  for substrates **1**, **2**, and **3**, and the total number of histidine residues  $N_{\text{His}}$ . Principal component analysis of this dataset showed that the first two principal components PC1 and PC2 explained 83% of the variability between the dendrimers (Figure 4). PC1 consisted mostly of substrate binding ( $1/K_{\text{M}}$ ) for each of the three substrates and  $N_{\text{His}}$ , and PC2 described mostly the catalytic rate constants  $k_{\text{cat}}$  for the three substrates.

(17) *Introduction to Multivariate Analysis*; Chatfield, C., Collins, A. J., Eds.; Chapman and Hall Ltd.: London, UK, 1983.

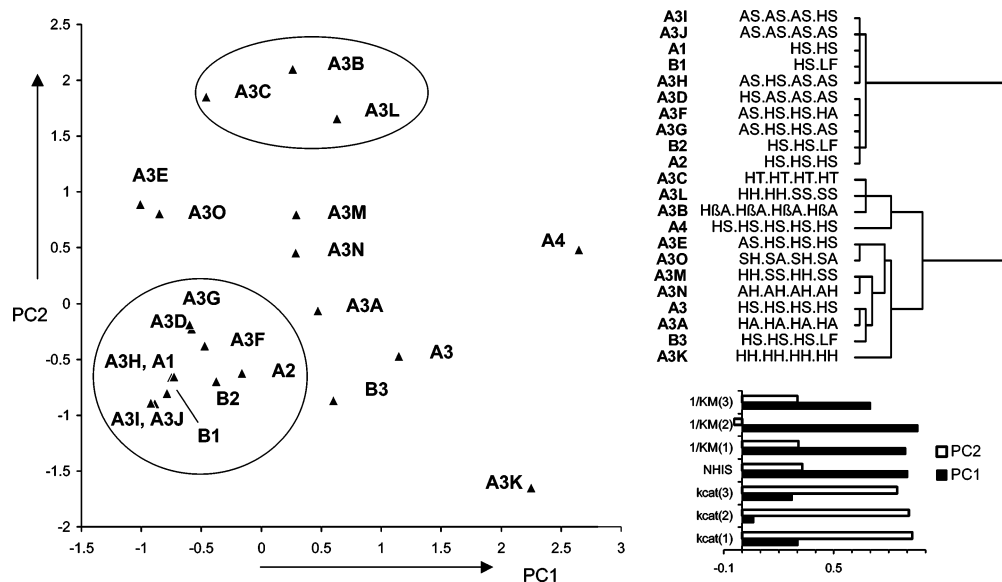


**FIGURE 4.** Principal component (PC) analysis of peptide dendrimers **A1–4**, **B1–3**, and **A3A–A3O** according to catalytic parameters  $k_{\text{cat}}$  and  $1/K_M$  for substrates **1–3** and total number of histidines  $N_{\text{His}}$ . Main plot: PC plot according to PC1 and PC2, which explains 84% of the observed variability. Clusters defined by hierarchical clustering are marked in circles. Upper right: Dendrogram of similarities between dendrimers (Ward's method with squared euclidean distances). Lower right: Loading of the principal components PC1 and PC2. The variables are normalized to an average value of 0 and a standard deviation of 1 prior to processing.

Cluster analysis of the dendrimer series defined groups of similar dendrimers well visible in the principal component plot (Figure 4). A first group was formed by dendrimers featuring modest substrate binding and catalytic properties (lower left plot in Figure 4). These dendrimers all contained 8 or fewer histidine residues. A second group was formed by the original sequence **A3** and several close analogues including the more weakly active hydrophobic core analogue **B3**, the Ser-Ala mutants **A3A** and **A3N**, and the permuted sequence **A3M** (center plot in Figure 4). Dendrimers **A3E** and **A3O** formed a third group with relatively good catalytic rate constants  $k_{\text{cat}}$  but weak substrate binding (upper left plot in Figure 4). The whole histidine dendrimer **A3K** and the fourth generation His-Ser dendrimer **A4** stood out at high PC1 values by their particularly strong substrate binding associated with a much larger number of histidine residues (right plot in Figure 4). **A4** was highly catalytically active, while **A3K** was not. Finally, the three most active dendrimers, namely the Ser- $\beta$ Ala mutant **A3B**, the Ser-Thr mutant **A3C**, and the reshuffled His-Ser sequence **A3L**, appeared at high PC2 values denoting high catalytic rate constants  $k_{\text{cat}}$  (top center plot in Figure 4).

The fact that  $1/K_M$  is found together with  $N_{\text{His}}$  in PC1 indicates that the linear correlation between  $N_{\text{His}}$  and  $1/K_M$  is conserved throughout the dendrimers series. By contrast  $N_{\text{His}}$  is only weakly associated with PC2, which is composed of the catalytic rate constants  $k_{\text{cat}}$  for all three substrates (Figure 4). Indeed linear regression analysis shows that  $N_{\text{His}}$  correlates with  $1/K_M(\mathbf{1})$  ( $r^2 = 0.669$ ),  $1/K_M(\mathbf{2})$  ( $r^2 = 0.661$ ), and  $1/K_M(\mathbf{3})$  ( $r^2 = 0.660$ ), but not with  $k_{\text{cat}}(\mathbf{1})$  ( $r^2 = 0.290$ ),  $k_{\text{cat}}(\mathbf{2})$  ( $r^2 = 0.088$ ), or  $k_{\text{cat}}(\mathbf{3})$  ( $r^2 = 0.187$ ). The correlation between substrate binding and  $N_{\text{His}}$  suggests that a large part of the observed substrate binding can be attributed to the presence of histidine residues. On the other hand, the mere presence of histidine residues is clearly not sufficient to explain the occurrence of catalysis. The difference is striking when comparing the replacement of serine in **A3** by  $\beta$ -alanine (**A3B**) or threonine (**A3C**), which significantly increases catalytic efficiency, while the simple replacement for

alanine (**A3A**) has only a minor effect on the catalytic properties of the dendrimer.

**Further Evidence for the Involvement of Histidines in Substrate Binding.** The cluster analysis above clearly pointed to a primary role of histidine residues in substrate binding. The pH profile data with dendrimers **A3** and **A4** were therefore analyzed with respect to the pH dependence of  $K_M$ . Michaelis–Menten kinetics with butyrate **2** gave very low  $K_M$  values below pH 6.0 when measured in 20 mM Bis-tris (Bis(hydroxyethyl)-tris(hydroxymethyl)-aminomethane) or MES (morpholinoethane sulfonic acid) buffers, which only allowed the determination of  $k_{\text{cat}}$ . Substrate binding was found to be weaker in the presence of the trianionic citrate buffer (5 mM), allowing measurable  $K_M$  values below pH 5.5 to be obtained as well. The  $K_M$  values of substrate **2** with dendrimer **A3** in citrate buffer increased linearly from 33  $\mu\text{M}$  at pH 5.2 to 180  $\mu\text{M}$  at pH 6.0 in that buffer, while the catalytic rate constant showed a maximum around pH 5.5 as in the other buffer systems (Figure 5). The higher  $K_M$  values in citrate buffer and their pH dependence can be interpreted in terms of the citrate trianion competing against the substrate's sulfonate groups for binding to the dendrimer via salt bridge interactions with the protonated histidines, and are consistent with histidines being involved directly in substrate binding interactions.<sup>18</sup>

Similar binding interactions between sulfonate groups and protonated histidines might explain the competitive inhibition of dendrimer **A3** catalyzed hydrolysis of **2** observed with pyrene 1,3,6,8-tetrasulfonate **6** ( $\text{IC}_{50}(\mathbf{6}) = 200 \mu\text{M}$  at 200  $\mu\text{M}$  **2**, pH 5.5). Such interactions are presumably essential for substrate binding and might explain the absence of catalysis with fluorogenic substrates **8–10**, which have similar or higher chemical reactivities compared to the pyrene sulfonates **1–4**, but lack the negatively charged sulfonate groups.

(18) For ion pair in water: (a) Schmuck, C.; Heil, M.; Scheiber, J.; Baumann, K. *Angew. Chem., Int. Ed.* **2005**, *44*, 7208–7212. (b) Rensing, S.; Schrader, T. *Org. Lett.* **2002**, *4*, 2161–2164. (c) Hossain, M. A.; Schneider, H.-J. *J. Am. Chem. Soc.* **1998**, *120*, 11208–11209.



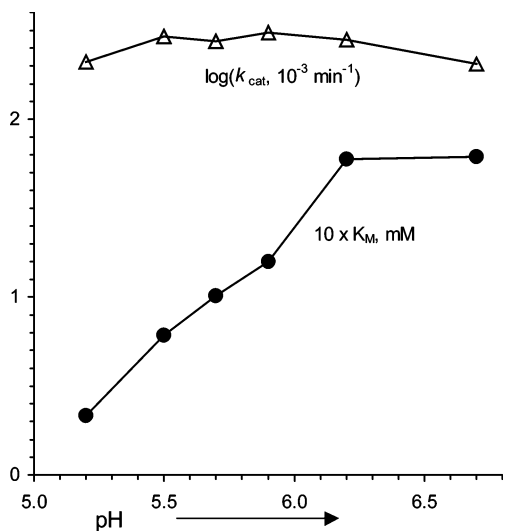


**FIGURE 5.** pH profile of catalytic parameters  $k_{\text{cat}}$  and  $K_{\text{M}}$  for dendrimer **A3** catalyzed hydrolysis of butyrate **2** in aqueous 5 mM citrate buffer. Conditions: 3.55  $\mu\text{M}$  **A3**, 10–1000 mM **2**, 25  $^{\circ}\text{C}$ , aqueous 5 mM citrate pH 4.9, 5.2, 5.5, 5.7, 5.9, 6.2, 6.7.

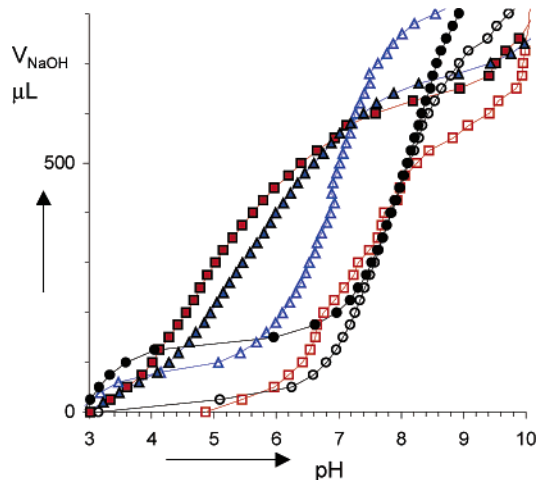


**FIGURE 6.** Determination of the apparent  $\text{p}K$  of histidine side chains by titration of the dendrimer TFA salts in the absence or presence of pyrene 1,3,6,8-tetrasulfonate **6**: 4-MeIm + 1.2 equiv of TFA ( $\bullet$ ), 4-MeIm + 1.2 equiv of TFA + 1.2 equiv of **6** ( $\circ$ ), **A3** ( $\blacktriangle$ ), **A3** + 5 equiv of **6** ( $\triangle$ ), and **A4** + 10 equiv of **6** ( $\square$ ). Conditions: 1 mM aqueous solution of dendrimers, and 40 mM 4-methylimidazole aqueous solution containing ca. 1.2 equiv of TFA, without or with pyrene 1,3,6,8-tetrasulfonate **6** were titrated with aliquots of 2 mM NaOH, 25  $^{\circ}\text{C}$ .

**Ionization State of Histidine Side Chains.** At any of the pH values, the extent of histidine protonation should directly influence binding of the trianionic substrates **1–3**. Furthermore, catalytic efficiency should depend on the percentage of free base present in the dendrimers assuming that the free base form is the key nucleophile or general base in catalysis (Scheme 3). The ionization state of histidine side chains as a function of pH was determined in peptide dendrimers **A3** and **A4** by direct titration of the trifluoroacetate salts of the dendrimers, as obtained from the preparative HPLC purification, with NaOH (Figure 6). The titration curve provided apparent  $\text{p}K$  ( $= \text{p}K_{\text{app}}$ ) values for histidine side chains (defined here as pH value for 50% ionization) of 5.7 for dendrimer **A3** and 5.0 for dendrimer **A4** (Table 5). This corresponds to approximately 30% free base

**TABLE 5.** Apparent  $\text{p}K$  of Histidine Side Chains<sup>a</sup>

compd	$\text{p}K_{\text{app}}$	$\text{p}K_{\text{app}}$ with <b>6</b>
4Me-Im	7.8	8.0
<b>A3</b>	5.7	6.8
<b>A4</b>	5.0	7.3

<sup>a</sup> Determined by titration of the trifluoroacetate salts with NaOH. Conditions: as in Figure 7.

form for histidines at the optimum pH of 5.5 for the dendrimer in the absence of bound substrate.

A similar titration was carried out in the presence of pyrene 1,3,6,8-tetrasulfonate **6** as a substrate analogue to mimic the dendrimer–substrate complex, using 1 equiv of **6** per substrate binding site as determined by ITC (Table 1). The histidine's  $\text{p}K_{\text{app}}$  in dendrimer **A3** increased by 1.1 pH units in the presence of **6**, and that of dendrimer **A4** by 2.25 pH units. This corresponds to less than 5% of histidines in the free-base form at the optimal pH of 5.5 for both dendrimers. By comparison, the apparent  $\text{p}K_{\text{app}}$  of 4-MeIm did not change significantly with and without tetrasulfonate **6**, indicating that the  $\text{p}K_{\text{app}}$ -shift effect was specific to the dendrimers.

The titration curves in the presence of tetrasulfonate **6** indicate 50% ionization of histidines at pH 6.8, which would be expected as the pH optimum for  $k_{\text{cat}}$  with a bifunctional mechanism rather than the observed pH 5.5. The pH optimum of 5.5 for  $k_{\text{cat}}$  might be explained in part by the fact that the number of binding sites decreases 4-fold between pH 5.5 and pH 7.0, as evidenced by ITC with dendrimer **A3** and product **5**, effectively reducing catalytic efficiency per dendrimer (Table 6).

**Ionic Strength Effects.** The effects of buffer, pH, and inhibitors discussed above clearly point to a strong electrostatic component in binding and catalysis. On the other hand, the ITC studies on the regular series **A1–A4** and the generally lower  $K_{\text{M}}$  values observed with the more hydrophobic substrate/dendrimer pairs suggest hydrophobic substrate–dendrimer interactions. The relative strength of electrostatic versus hydrophobic interactions was investigated by measuring the ionic strength dependence of catalysis. Electrostatic interactions are expected to be weakened at high ionic strength, while those depending on the hydrophobic effect should become stronger.<sup>19</sup>

Kinetic parameters were determined at the optimal pH of 5.5 from 0 to 500 mM KCl for dendrimer **A3** and substrates **1–3** (Figure 7A/B). The  $K_{\text{M}}$  values increased by approximately 10-fold across the KCl concentration range for all three substrates. The weaker substrate binding at high ionic strength supports an electrostatic component in substrate binding as inferred from the pH effects and inhibition by the pyrene tetrasulfonate **6** discussed above. Similar ionic strength effects on binding for substrate **2** were also observed with the hydrophobic core dendrimer **B3**, the weakly active whole histidine dendrimer **A3K**, and the highly efficient dendrimer **A3L** consisting of a whole histidine surface around a serine core (Figure 7C/D). These data provide further evidence that substrate binding in the dendrimer series depends strongly on electrostatic interactions between the sulfonate groups of the substrates and protonated histidine residues on the dendrimers.

The rate constant for the uncatalyzed reaction  $k_{\text{uncat}}$  increased approximately 2-fold for all three substrates from 0 to 500 mM KCl, as should be expected for an ionic transition state in a

(19) (a) Atkins, P. W. *Physical Chemistry*, 6th ed.; Oxford University Press: Oxford, UK, 1998. (b) Jencks, W. P. *Catalysis in Chemistry and Enzymology*; Dover Publications: New York, 1975.

TABLE 6. pH Dependence of the Calorimetric Titration of **5** Added to A3<sup>a</sup>

dendrimer	ligand	pH	<i>n</i>	<i>K</i> <sub>a</sub> (×10 <sup>4</sup> M <sup>-1</sup> )	Δ <i>H</i> <sub>a</sub> (kcal/mol)	Δ <i>G</i> <sub>a</sub> (kcal/mol)	Δ <i>S</i> <sub>a</sub> (cal/mol/K)
A3	5	5.0	3.77(±0.09)	3.23(±0.51)	-9.26(±0.29)	-25.89(±0.39)	55(±2)
A3	5	5.5	4.78(±0.43)	0.29(±0.05)	-8.89(±1.07)	-19.91(±0.43)	37(±5)
A3	5	6.0	3.14(±0.14)	0.89(±0.11)	-6.86(±0.40)	-22.69(±0.31)	53(±2)
A3	5	7.0	1.34(±0.93)	0.21(±0.05)	-11.00(±0.67)	-19.10(±0.65)	27(±4)

<sup>a</sup> Conditions: A3 0.1 mM, **5** 10 mM; buffers MES pH 5.0 (20 mM), citrate pH 5.5 (5 mM), Bis Tris pH 6.0 (20 mM), HEPES pH 7.0 (20 mM) at 27 °C

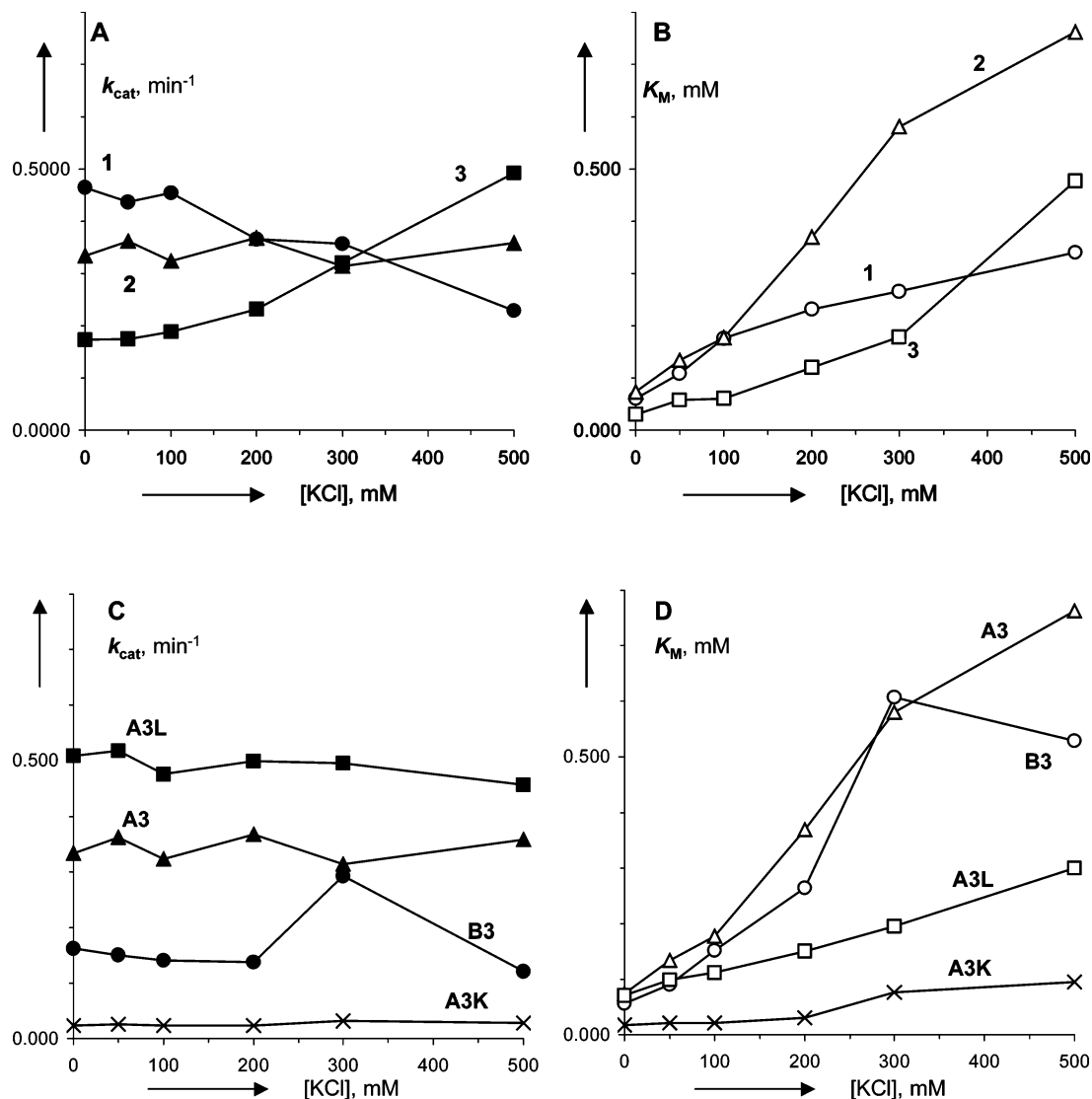


**FIGURE 7.** Ionic strength effects on dendrimer-catalyzed ester hydrolysis. (A, B) Catalytic parameters for dendrimer A3 catalyzed hydrolysis of 8-acyloxypropylene 1,3,6-trisulfonates **1** (acetate), **2** (butyryl), and **3** (nonanoyl) as a function of KCl concentration. (C, D) Catalytic parameters for the hydrolysis of butyrate **2** with dendrimers A3, A3K, and A3L. Conditions: 10–1000 μM ester, 3.55 μM dendrimers A3, A3K, and A3L, in aqueous 5 mM citrate pH 5.5 containing 0, 5, 10, 50, 100, 200, 300, 500 mM KCl, 26 °C.

more polar medium in the absence of interactions with a catalyst. By contrast the rate constant  $k_{\text{cat}}$  decreased by 2-fold with the acetate ester substrate **1** (Figure 7A). This effect is consistent with a specific transition state stabilizing dendrimer–substrate interaction of electrostatic nature, for example the stabilization of the oxyanion by a protonated histidine residue (Scheme 3). However, the  $k_{\text{cat}}$  values were independent of ionic strength with the butyrate ester **2** (Figure 7A/C) and increased with the nonanoate ester **3** (Figure 8A). This effect probably reflects

additional catalytically productive dendrimer–substrate interactions of hydrophobic nature involving the substrate’s acyl chain with these more hydrophobic substrates.

**Comparison with Enzymes and Enzyme Models.** Enzymes are macromolecular catalysts acquiring activity and selectivity from the interplay between amino acid side chains and optional cofactors in the folded state of the protein. Hallmarks of enzyme catalysis are selective substrate binding and catalysis in aqueous environment.<sup>20</sup> The esterase peptide dendrimers discussed here

address the problem of de novo enzyme design, which strives to construct functional protein-like structures from first principles.

The key advantage of our dendrimer approach is a robust and simple solid-phase synthesis approach. Thus, only 11 coupling steps are necessary to prepare third-generation peptide dendrimers containing 37 amino acids, which greatly facilitates the preparation of analogues. We have recently shown that the synthesis is also suitable for split-and-mix synthesis and allows active dendrimers to be discovered by screening combinatorial libraries.<sup>21</sup> The peptide dendrimers reported here show remarkable catalytic efficiencies up to  $k_{\text{cat}}/k_{\text{uncat}} = 90\,000$  for the Thr-Ser mutant **A3C**. This corresponds to 18 000 per catalytic site assuming three histidine residues per catalytic site as determined by ITC, among the best enzyme models reported to date in terms of catalytic efficiency.

Previous enzyme models based on SPPS for synthesis used folding linear peptides. Johnsson et al. reported a catalytic  $\alpha$ -helical peptide accelerating the decarboxylation of oxaloacetate using three catalytic lysine residues with  $k_{\text{cat}}/k_{\text{uncat}} = 600$ .<sup>22</sup> Broo et al. have reported a designed  $\alpha$ -helix bundle displaying multiple histidine side chains capable of hydrolyzing nitrophenyl esters with catalytic proficiency  $k_{\text{cat}}/K_{\text{M}} = 230$  relative to 4-methylimidazole at pH 5.1.<sup>10c</sup> SPPS has been used to prepare combinatorial libraries of short linear peptides, and has yielded efficient catalysts for a variety of reactions.<sup>23</sup> These catalytic peptides contain some side chain protected amino acids, and show activity and selectivity in organic solvents but not in water. Other chemical synthetic strategies to artificial enzymes include the modification of macromolecules (e.g., cyclodextrins) and dendrimers (PAMAM, PPI), emphasizing the preparation of single macromolecular models without regards to enabling evolution and functional selection. Breslow and Schmuck reported a rate acceleration of  $k_{\text{cat}}/k_{\text{uncat}} = 120$  for the hydrolysis of nitrophenyl phosphate catalyzed by a bis-imidazole substituted  $\beta$ -cyclodextrin.<sup>10j</sup> A PPI-based polyimidazole catalyst showed only modest esterase activities with nitrophenyl acetate.<sup>10e-i</sup>

The peptide dendrimer approach may also be compared with catalytic antibody technology.<sup>24</sup> Esterase antibodies are among the best reported antibodies with rate accelerations  $k_{\text{cat}}/k_{\text{uncat}}$  in the range  $10^3$ – $10^5$ , comparable with our peptide dendrimers, although the antibodies are much larger (50 kDa per catalytic

site) than our peptide dendrimers (4.5 kDa). A further approach to artificial enzyme design consists of combining noncatalytic proteins with catalytically active cofactors. For example, Distefano et al. reported enantioselective reductive amination processes in a lipid-binding protein modified with a pyridoxamine cofactor.<sup>25</sup> Ward et al. have used streptavidin combined achiral metal complexes for enantioselective catalytic hydrogenations and oxidations.<sup>26</sup> In these systems the protein shell is used for providing selectivity, but does not provide large rate enhancements over the reaction of the cofactor or metal complex alone, precluding a direct comparison with our dendrimers in terms of efficiency.

De novo enzyme design has also been approached by using algorithms to discover folding peptides by computational or recombinant DNA methods.<sup>5</sup> Thus, computational design generated an esterase active site at the surface of thioredoxin with a single histidine residue that catalyzed the hydrolysis of nitrophenyl acetate with  $k_{\text{cat}}/k_{\text{uncat}} = 180$  and  $K_{\text{M}} = 0.17$  mM.<sup>4f</sup> Wey and Hecht have discovered a properly folded four-helix bundle from a designed genetic library, and reported esterase activities for nitrophenyl acetate after introduction of surface histidine residues, with  $k_{\text{cat}}/k_{\text{uncat}} = 8700$ , but no observable substrate binding ( $K_{\text{M}} = 3$  mM).<sup>4j</sup>

## Conclusion

Peptide dendrimers **A1**–**A4** composed of the repeating dendron Dap-His-Ser catalyze the hydrolysis of 8-acyloxypyrene 1,3,6-trisulfonates **1**–**3** in aqueous buffer and show a strong positive dendritic effect in catalytic proficiency. The mechanism of the dendrimer-catalyzed ester hydrolyses is best understood in terms of bifunctional catalysis involving a free-base histidine acting as nucleophile or general base, together with a protonated histidine stabilizing the oxyanion intermediate, as evidenced by pH–rate profile data showing a maximum activity at pH 5.5.

Mutant dendrimers were prepared to examine the dependence of catalytic activity on amino acid composition. Seventeen dendrimers **B1**–**O4** incorporating hydrophobic residues at the core as well as negatively charged residues were examined to provide more protein-like catalysts. These dendrimers were catalytically less efficient than the parent series **A1**–**A4**. In a second approach a series of 15 close analogues of the third generation dendrimer **A3** were prepared by parallel synthesis. The dendrimers were investigated for their catalytic properties for the hydrolysis of acyloxypyrene trisulfonates **1**–**3**, which proved to be the only reactive substrate type for this class of dendrimers. Exchanging the serine residues in **A3** against  $\beta$ -alanine (**A3B**) or threonine (**A3C**), or reshuffling histidine and serine residues between the different positions (**A3L**), led to catalytically more efficient dendrimers. **A3C** showed the highest rate acceleration for a third-generation dendrimer with  $k_{\text{cat}}/k_{\text{uncat}} = 90\,000$ , corresponding to  $k_{\text{cat}}/k_{\text{uncat}} = 18\,000$  per catalytic site, a 10-fold improvement over the original dendrimer **A3**. On the other hand **A3B** showed the highest specific reactivity enhancement of  $(k_{\text{cat}}/K_{\text{M}})/k_2 = 91\,000$  over the

(20) (a) Stryer, L. *Biochemistry*; WH Freeman and Company: New York, 1999. (b) Fersht, A. *Structure and Mechanism in Protein Science*; WH Freeman and Company, New York, 1999.

(21) (a) Clouet, A.; Darbre, T.; Reymond, J.-L. *Angew. Chem., Int. Ed.* **2004**, *43*, 4612–4615. (b) Clouet, A.; Darbre, T.; Reymond, J.-L. *Biopolymers (Peptide science)* **2006**, *84*, 114–123.

(22) Johnsson, K.; Allemann, R. K.; Widmer, H.; Benner, S. A. *Nature* **1993**, *365*, 530–532.

(23) (a) Jarvo, E. R.; Miller, S. J. *Tetrahedron* **2002**, *58*, 2481–2495. (b) Vasbinder, M. M.; Jarvo, E. R.; Miller, S. J. *Angew. Chem., Int. Ed.* **2001**, *40*, 2824–2827. (c) Wennemers, H.; Conza, M.; Nold, M.; Krattiger, P. *Chem. Eur. J.* **2001**, *7*, 3342–3347. (d) Sigman, M. S.; Jacobsen, E. N. *J. Am. Chem. Soc.* **1998**, *120*, 4901–4902. (e) Tang, Z.; Jiang, F.; Yu, L.-T.; Cui, X.; Gong, L.-Z.; Mi, A.-Q.; Jiang, Y.-Z.; Wu, Y.-D. *J. Am. Chem. Soc.* **2003**, *125*, 5262–5263. (f) Tang, Z.; Jiang, F.; Cui, X.; Gong, L.-Z.; Mi, A.-Q.; Jiang, Y.-Z.; Wu, Y.-D. *Proc. Natl. Acad. Sci. U.S.A.* **2004**, *101*, 5755. (g) Martin, H. J.; List, B. *Synlett* **2003**, 1901. (h) Kofoed, J.; Nielsen, J.; Reymond, J.-L. *Bioorg. Med. Chem. Lett.* **2003**, *13*, 2445. (i) For one example in water see: Berkessel, A.; Héroult, D. A. *Angew. Chem., Int. Ed.* **1999**, *38*, 102–105.

(24) (a) Lerner, R. A.; Benkovic, S. J.; Schultz, P. G. *Science* **1991**, *252*, 659–667. (b) Schultz, P. G.; Lerner, R. A. *Acc. Chem. Res.* **1993**, *26*, 391–395. (c) Schultz, P. G.; Lerner, R. A. *Science* **1995**, *269*, 1835–1842. (d) MacBeath, G.; Hilvert, D. *Chem. Biol.* **1996**, *3*, 433–445.

(25) (a) Kuang, H.; Distefano, M. D. *J. Am. Chem. Soc.* **1998**, *120*, 1072–1073. (b) Qi, D.; Tann, C.-M.; Haring, D.; Distefano, D. *Chem. Rev.* **2001**, *101*, 3081–3111. See also: Levine, H. L.; Kaiser, E. T. *J. Am. Chem. Soc.* **1978**, *100*, 7670–7677 for a flavin modified papain system.

(26) (a) Skander, M.; Humbert, N.; Collot, J.; Gradinau, J.; Klein, G.; Loosli, A.; Sausser, J.; Zocchi, A.; Gilardoni, F.; Ward, T. R. *J. Am. Chem. Soc.* **2004**, *126*, 14411–14418. (b) Thomas, C. M.; Ward, T. R. *Chem. Soc. Rev.* **2005**, *34*, 337–46.

reference catalyst 4-methylimidazole, which amounts to 18 200-fold higher reactivity per catalytic site. The higher catalytic activity of dendrimer **A3B**, **A3C**, and **A3L** compared to **A3** might reflect favorable structural changes upon mutations resulting in a more favorable relative placement of histidines optimizing bifunctional catalysis.

Statistical analysis of the rate data showed that the number of histidine residues per dendrimer was correlated with its binding affinity  $1/K_M$  to the substrates, but did not predict the catalytic rate constants  $k_{cat}$ , which are strongly structure dependent. Analysis of pH and ionic strength effects and ITC data indicate that substrate binding depends on electrostatic interactions between the substrate's sulfonate groups and protonated histidine residues combined with hydrophobic interactions between the substrate's acyl chain and the dendrimer.

Peptide dendrimers such as those reported here are very attractive as artificial protein models. The dendrimers are well-behaved and show excellent stability. Most importantly, the synthesis of peptide dendrimers proceeds in excellent yields and uses standard solid-phase synthesis protocols readily amenable to automated synthesis. The present study illuminates a complex structure–function relationship in catalytic peptide dendrimers in which the nature and position of the amino acids strongly modulate substrate binding and catalysis. Experiments toward the discovery of enantioselective esterase peptide dendrimers by a combinatorial chemistry approach are in progress.<sup>21</sup>

## Experimental Part

**1. Dendrimer Synthesis.** Peptide dendrimers were synthesized with the Fmoc strategy, according to standard solid-phase procedure, as described in the Supporting Information.

**1.a. General Procedure for Dendrimer Synthesis.** Eluent A: water and TFA (0.1%); eluent B: acetonitrile, water and TFA (3/2/0.1%).

The synthesis of dendrimers **A1–O4** has been achieved following procedure A. **Procedure A:** The resin NovaSyn TGR (0.25 mmol/g) was acylated with each amino acid or diamino acid (3 equiv) in the presence of BOP (3 equiv) and DIEA (5 equiv) for 30 min, 1 h after the first generation, 2 h after the second generation, 3 h after the third generation, and 5 h after the fourth generation. After each coupling the resin was successively washed with DMF, MeOH, and  $\text{CH}_2\text{Cl}_2$  (3 $\times$  with each solvent), then checked for free amino groups with the TNBS test. If the TNBS test indicated the presence of free amino groups, the coupling was repeated. In case of uncertainty in the completion of the coupling, the potential remaining free amino groups were capped with acetic anhydride/ $\text{CH}_2\text{Cl}_2$  for 10 min. The Fmoc protecting groups were removed with a solution of 20% piperidine in DMF (2 $\times$  10 min) and the solvent was removed by filtration. At the end of the synthesis, the resin was acylated with acetic anhydride/ $\text{CH}_2\text{Cl}_2$  (1:1) for 1 h. The resin was dried and the cleavage was carried out with TFA/anisole/1,2-ethanedithiol/ $\text{H}_2\text{O}$  (94:5:1:1) for 4 h. The peptide was precipitated with methyl *tert*-butyl ether then dissolved in a water/acetonitrile mixture. All dendrimers were purified by preparative HPLC.

**((Ac-His-Ser)<sub>2</sub>DapHis-Ser)<sub>2</sub>DapHis-Ser)<sub>2</sub>DapHis-SerNH<sub>2</sub> (A3):** Starting with 200 mg of NovaSyn TGR resin (0.25 mmol/g), the sequence **((His-Ser)<sub>2</sub>BHis-Ser)<sub>2</sub>BHis-Ser)<sub>2</sub>BHis-SerNH<sub>2</sub>** was prepared. Half of the resin was acetylated and the product cleaved from the resin and purified by preparative HPLC to give **A3** as a colorless foamy solid (34.2 mg, 22.7%). MS (ES+) calcd for  $\text{C}_{172}\text{H}_{242}\text{N}_{75}\text{O}_{60}$  [M + H]<sup>+</sup> 4317.81, found 4318.13.

The synthesis of dendrimers **A3A** to **A3O** has been achieved by Dr. Quang N'Guyen (Chem Speed AG) following procedure B. **Procedure B: Automated Solid-Phase Dendrimer Synthesis.** The

synthesis was carried out in a PSW1100 peptide synthesizer (Chemspeed AG). The resin NovaSyn TGR (0.23 mmol/g) was acylated with each amino acid or diamino acid (0.5 M in DMF, 3 equiv) in the presence of HBTU/HOBt (0.5 M in DMF, 3 equiv) and *N*-methylmorpholine (1.0 M in DMF, 6 equiv) for 1 (first generation), 2 (second generation), and 4 h (third generation). Each coupling was repeated twice. The Fmoc protecting group was removed with a solution of 20% piperidine in DMF (3 $\times$  10 min) and the solvent was removed by filtration. After each coupling and Fmoc-deprotection the resin was washed with DMF (3 $\times$ ). At the end of the synthesis, the resin was acylated with acetic anhydride/ $\text{CH}_2\text{Cl}_2$  (1:1) for 1 h. The resin was washed with  $\text{CH}_2\text{Cl}_2$  and dried under reduced pressure. The resin was dried and the cleavage was carried out with TFA/TIS/ $\text{H}_2\text{O}$  (94:5:1) for 4 h. The peptide was precipitated with methyl *tert*-butyl ether then dissolved in a water/acetonitrile mixture. All dendrimers were purified by preparative HPLC.

**((Ac-His-Thr)<sub>2</sub>DapHis-Thr)<sub>2</sub>DapHis-Thr)<sub>2</sub>DapHis-ThrNH<sub>2</sub> (A3C):** Starting with 100 mg of NovaSyn TGR resin (0.23 mmol/g), the dendrimer **A3C** was obtained as a colorless foamy solid after cleavage from the resin and preparative RP-HPLC purification (19.1 mg, 13.3%). MS (ES+) calcd for  $\text{C}_{187}\text{H}_{272}\text{N}_{75}\text{O}_{60}$  [M + H]<sup>+</sup> 4528.05, found 4528.75.

Purification conditions and characterization of all dendrimers is given in the Supporting Information.

**2. Assays and Kinetic Measurements.** Assays were followed in individual wells of round-bottom polystyrene 96-well plates using a fluorescence detector with preset values of the excitation and emission wavelengths corresponding to the measured substrate. All pipetting manipulations were done by hand with single pipets. The measurement temperature inside the instrument was 26.5 °C. Kinetic experiments were followed for 2–12 h. Fluorescence data were converted to product concentration by means of a calibration curve.

**2.a. Typical Measurement of Apparent Rate Enhancements.** In a typical experiment, 20  $\mu\text{L}$  of aqueous buffer were first added in a well, followed by 2.5  $\mu\text{L}$  of the dendrimer solution (typically 0.05 mM in aq buffer, final concentration in the well was 5  $\mu\text{M}$ ), and finally 2.5  $\mu\text{L}$  of substrate solution (typically 2 mM in acetonitrile/water 1/1, final concentration in the well was 200  $\mu\text{M}$ ). The rate observed under these conditions is the apparent rate  $V_{app}$ .  $V_{un}$  is the rate observed with 22.5 mL of aqueous buffer and 2.5  $\mu\text{L}$  of substrate solution (2 mM in acetonitrile/water 1/1, final concentration in the well was 200  $\mu\text{M}$ ). The observed rate enhancement is defined as  $V_{net}/V_{un}$ .

**2.b. Michaelis–Menten Plots.** Michaelis–Menten plots were obtained from the linear double reciprocal plot of  $1/V_{net}$  versus  $1/[S]$  (where  $V_{net} = V_{app} - V_{un}$  and  $[S]$  is the substrate concentration) measured with dendrimers ( $V_{app}$ ) or without dendrimer ( $V_{un}$ ) in aqueous buffer. In a typical experiment, 20  $\mu\text{L}$  of aqueous buffer were first added in a well, followed by 2.5  $\mu\text{L}$  of the dendrimer solution (typically 35.5  $\mu\text{M}$  in aqueous buffer, final concentration in the well was 3.55  $\mu\text{M}$ ), and 10, 20, 30, 40, 60, 80, 100, 200, 400, 600, 800, and 1000  $\mu\text{M}$  substrate in acetonitrile/water 1/1. Initial reaction rates  $V_{app}$  and  $V_{un}$  were obtained from the steepest part observed in the curve that gives fluorescence versus time, typically during the first 2000 s for  $V_{app}$  and during the first 4000 s for  $V_{un}$ . The rate constant  $k_{uncat}$  without catalyst was calculated from the slope of the linear curve that gives  $V_{un}$  (as product concentration per time) versus substrate concentration  $[S]$ .

**2.c.  $k_2$ (4-methylimidazole).** A stock solution of 40 mM of 4-methylimidazole was prepared, buffered in the desired aqueous buffer. The reaction rate with 4-methylimidazole (4-MeIm) was obtained under the same conditions as above with 40, 60, 80, 100, 200, 300, 400, 500, 800, and 1000  $\mu\text{M}$  4-MeIm, 200  $\mu\text{M}$  substrate in acetonitrile/water 1/1, and aq buffer. The second-order rate constant  $k_2$  was calculated from linear regression of the experimentally measured pseudo-first-order rate constants  $k'$  as a function

of 4-MeIm concentrations. The second-order rate constant  $k_2$  is given by  $k_2 = k'/[S]$ , where  $[S]$  indicates the concentration of substrate.

**2.d. Inhibition with Pyrene 1,3,6,8-Tetrasulfonate.** The inhibition constant  $K_1$  was obtained from the linear reciprocal plot of  $1/V_{\text{net}}$  vs  $[I]$  measured similarly with (final concentrations)  $5 \mu\text{M}$  dendrimer and  $200 \mu\text{M}$  substrate ( $V_{\text{app}}$ ) and 0, 10, 20, 40, 60, 80, 100, 200, 400, 600, 800, and  $1000 \mu\text{M}$  pyrene 1,3,6,8-tetrasulfonate, 5 mM citrate pH 5.5, 26.5 °C.

**2.e. Ionic Strength.** Ionic strength effect, i.e., initial velocities of product formation as a function of KCl concentration, was studied with Michaelis–Menten plots obtained as described above. Conditions, if not varied as indicated:  $3.55 \mu\text{M}$  dendrimer (final concentration in the well), 10, 20, 30, 40, 60, 80, 100, 200, 400, 600, 800, and  $1000 \mu\text{M}$  substrate (final concentration in the well), and 5 mM citrate buffer pH 5.5 containing KCl (respectively 0, 5, 10, 50, 100, 200, 300, and 500 mM). For each buffer, the linear relationship between fluorescence and product concentration was determined with a calibration curve.

**2.f.  $pK_a$  Determination.** The histidine residues of the dendrimers were titrated by adding aliquots ( $20 \mu\text{L}$ ) of 2 mM NaOH in a 1

mM aqueous solution of dendrimer (or 40 mM 4-methylimidazole aqueous solution containing ca. 1.2 equiv of TFA) without or with pyrene 1,3,6,8-tetrasulfonate **6**, with respect to the number of binding sites as determined by isothermal titration calorimetry (5 equiv of **6** was added to **A3A**, 10 equiv of **6** was added to **A4**). The experiments were repeated and gave reproducible values within 10% error.

**Acknowledgment.** This work was financially supported by the University of Berne, the Swiss National Science Foundation, the COST program D25, and the European Marie Curie Training Network IBAAC.

**Supporting Information Available:** Procedures for dendrimer synthesis, HPLC, and MS data of all dendrimers synthesized, procedures for kinetic measurements, and ITC and pH studies. This material is available free of charge via the Internet at <http://pubs.acs.org>.

JO060273Y